Identification of mantle peridotite as a possible Iapetan ophiolite sliver in south Shetland, Scottish Caledonides

James M.D. Day[1*], Brian O'Driscoll[2], Rob A. Strachan[3], J. Stephen Daly[4,5], Richard J. Walker[6]

[1]Geosciences Research Division, Scripps Institution of Oceanography, La Jolla, CA 92093-0244, USA
[2]School of Earth, Atmospheric and Environmental Sciences (SEAES), University of Manchester, Manchester, M13 9PL, UK
[3]School of Earth and Environmental Science, University of Portsmouth, Portsmouth PO1 2UP, UK
[4]UCD School of Earth Sciences, University College Dublin, Belfield, Dublin 4, Ireland
[5]Irish Centre for Research in Applied Geosciences (icrag-centre.org)
[6]Department of Geology, University of Maryland, College Park, MD 20742, USA
*Corresponding author: jmdday@ucsd.edu

The Journal of the Geological Society of London, Special (JGS2016-074)

Abstract *(95 words)*

The Neoproterozoic Dunrossness Spilite Subgroup (DSS) of south Shetland, Scotland, has been interpreted as a series of komatiitic and mafic lava flows formed in a marginal basin in response to Laurentian continental margin rifting. We show that ultramafic rocks previously identified as komatiites are depleted mantle peridotites that experienced seafloor hydrothermal alteration. The presence of positive Bouguer gravity and aeromagnetic anomalies extending from the DSS northward to the Shetland Ophiolite Complex suggest instead that these rocks may form part of an extensive ophiolite sliver, obducted during Iapetus Ocean closure in a fore-arc setting.

Keywords: Shetland; ophiolite; peridotite; komatiite; osmium isotopes; Iapetus

Supplementary Information, including methods, supplementary figures and tabulated data accompanies this JGS Special Article

Ophiolites are fragments of oceanic lithosphere tectonically incorporated into continental margins (Dewey & Bird, 1971; Coleman, 1977; Nicolas, 1989). Identification of ophiolites is important for revealing ocean basin evolution during Wilson cycles (e.g., Dilek & Furnes, 2011)

and for understanding oceanic crust formation and mantle heterogeneity (e.g., O'Driscoll et al., 2012; 2015). The Penrose definition of an ophiolite (Anonymous, 1972, p. 24), describes a distinctive assemblage comprising, from bottom to top, tectonized peridotites, cumulate ultramafic rocks overlain by layered gabbros, sheeted basaltic dykes, and a volcanic sequence. This complete assemblage is found in few ophiolite complexes, with most being identified on two or more of these characteristic traits (Dilek & Furnes, 2011). For example, within the Scottish Caledonides, the Shetland Ophiolite Complex (SOC) comprises tectonized mantle peridotite, cumulate peridotite and gabbros (Flinn & Oglethorpe, 2005).

Here, we suggest that the Neoproterozoic(?) Dunrossness Spilite Subgroup (DSS) in south Shetland may be part of an ophiolite. The DSS has been described as a volcaniclastic sequence of ultramafic and mafic rocks, including ultramafic (>22 wt.% MgO) "komatiite" (Flinn, 1967; Flinn & Moffat, 1985; Flinn, 2007; Flinn et al., 2013). As a Neoproterozoic komatiite occurrence, the DSS would represent an anomalously young example of komatiite magmatism. New data for ultramafic samples reveal that they are depleted mantle peridotites, with traits distinct from komatiite. This re-interpretation of the DSS and its possible correlation with the SOC from geophysical anomalies suggests that a fuller ophiolite sequence crops out more extensively in Shetland than hitherto recognized. There are also implications for the tectonic provenance of the ophiolite, as some models rested on identification of komatiite in the DSS (Flinn & Moffat, 1985; Flinn 2007).

Geological Setting and Sample Details

The DSS has been interpreted as the highest stratigraphic portion of the Laurentian Dalradian succession of Shetland (Flinn et al., 1972), occurring at a similar stratigraphic level to the Clift Hills Group of Unst, beneath the SOC. The DSS mainly comprises mafic and ultramafic rocks interpreted to have formed in a sub-marine environment, and that lie above Dalradian metapelites of the Dunrossness Formation (**Figure 1**). The geological context during the genesis of the DSS is one of development and closure of the Iapetus Ocean after prolonged deposition of the Dalradian Supergroup from ~730 Ma to as late as 470 Ma (Strachan et al., 2002, 2013). Iapetan-aged ophiolite obduction onto and along the southeast margin of the Grampian Terrane in

the Scottish and Irish Caledonides (**Figure 1**) occurred in response to Grampian arc-continent collision at ~480 Ma (e.g., Dewey & Ryan 1991; Crowley & Strachan 2015).

The mafic and ultramafic rocks of the DSS have been interpreted as marine volcanic and volcaniclastic rocks formed in a rift setting (Flinn, 1967; 2007; Flinn & Moffat, 1985; 1986; Flinn et al., 2013). The DSS can be broadly separated into three main sub-units; a lower phyllitic formation, an intermediate ultramafic unit, and an upper mafic unit that contains pillow lavas (**Figure 1**). For the most ultramafic (and serpentinized) unit, Flinn and co-workers argued for a volcaniclastic breccia origin, where blocks of materials with 'spinifex-like texture' occur (Flinn & Moffat, 1985). Nearly-spherical to sub-lenticular bodies of hornblende-bearing gabbro also occur within the serpentinite, along with veins of sodic 'keratophyre' (an albite felsite). Associated interbedded mudstones and sandstones have been interpreted as deep marine turbidites. (Flinn, 2007).

Re-investigation of the contacts of the DSS with the underlying Dalradian pelites to the west indicates that these are invariably highly tectonised (see also Flinn et al., 2013). Where the contact is exposed on the coast at Lamba Taing, the lowest 30-40m of the DSS comprises lenticular tectonic slices of ultramafic lithologies, metagabbro and phyllite. The lowermost ultramafic exposures have sharp contacts with mylonitic phyllites of the Dunrossness Group. The location from which we sampled is a lens of serpentinite that crosses the A970 road and intersects the coast, lying parallel to the foliation in the spilitic and volcaniclastic rocks (**Figure 1**). The serpentinite has been variably replaced (steatitized) and veined by talc.

Results

The investigated samples contain large (>2 cm) rounded to elongated polycrystalline aggregates of orange-brown magnesite embedded within a matrix of blue-grey fibrous talc (*Figure S1*). Accessory Cr-spinel and associated secondary Fe-Cr-oxide/hydroxide minerals are disseminated throughout the rock, both within talc and magnesite. The talc-magnesite sample has a high loss on ignition (LOI = 19.7 wt.%), consistent with significant abundances of volatile species (e.g., CO_2, H_2O), as well as the steatitization of serpentinite. Anhydrous corrected major-

element abundances (methods described in *Supplementary Materials*) indicate low abundances of Al_2O_3 (0.2 wt.%), CaO (1.6 wt.%), Na_2O and K_2O, but high MgO and SiO_2 (*Table S1*). The samples also contain high concentrations of Ni (1600-2400 μg g^{-1}) and Cr (1400-3750 μg g^{-1}). These compositions are similar to the major and minor element concentrations reported by Flinn & Moffat (1985) for their 'komatiite' rock. The Dunrossness samples lie at the depleted end of SOC harzburgite samples for Al_2O_3 versus Fe_2O_3 and V, and within the range of SOC dunites (*Figure S2*).

Whole-rock analyses of three talc-magnesite samples *(Figure S3)* are systematically depleted in most incompatible trace elements, with respect to the primitive mantle composition, with notable exceptions for Ba, W and Pb. Relative enrichments are evident for Sr, Eu, U, Ta and Cs, with extreme relative depletions for Rb, Th, Nb, Zr, Hf and Ti. Rare earth elements (REE) are <0.1 × primitive mantle and have slightly elevated light REE compared with the heavy REE (La/Yb = 2.7-3.3). REE patterns in the talc-magnesite samples are distinct from harzburgites and dunites from the Iapetan-aged Shetland and Leka (Norway) ophiolites (O'Driscoll et al., 2015; authors' unpublished data), having slightly higher overall REE abundances, and a relatively flat pattern lacking depletion in the middle REE, and a positive Eu anomaly.

Highly siderophile element abundances (HSE: Os, Ir, Ru, Pt, Pd, Re) are in the upper range of those for SOC dunites and harzburgites, with relative Pt, Pd and Re enrichments (Pd/Os = 8.8-11.8; Pt/Os = 6.4-11.8; Ru/Os = 1.2-2.3; Ir/Os = 1.3-1.7) (**Figure 2**). Talc-magnesite $^{187}Os/^{188}Os$ ratios range between 0.1227 and 0.1243, corresponding to γOs values of -2.5 to -3.8. Values of $^{187}Re/^{188}Os$ range from 0.26 to 2.1. Samples are not isochronous, but are in the range of $^{187}Os/^{188}Os$ for SOC harzburgites, implying recent Re addition to S 2009 b/c samples (**Figure 3**).

Discussion and conclusions

Steatitization and serpentinization of mantle peridotite?

The anhydrous bulk-composition of the DSS talc-magnesite samples is similar to peridotite that has experienced extensive serpentinization and metasomatism. The DSS samples

have also been steatitized but are otherwise similar to that of the sample in Flinn & Moffat (1985), which was reportedly not steatitized. One principal difference is that the steatitized sample reported here has much lower Mg. This difference is due to Mg-loss or Si-gain during localized steatitization within the DSS ultramafic rocks. Significant apparent Mg-loss from peridotite occurs in both marine (e.g., Janecky & Seyfried, 1986; Snow & Dick, 1995) and terrestrial environments (e.g., Alexander, 1988) due to hydrothermal and weathering processes. The bulk compositions of our sample and that of Flinn & Moffat (1985) are therefore consistent with peridotite protoliths, an observation supported by similarity in bulk composition between the DSS ultramafic rocks and SOC ultramafic rocks on Unst and Fetlar. Enrichments in Sr, Ba, Pb, U and Cs, the light REE and Eu all indicate extensive seafloor alteration of the talc-magnesite samples. Notably, the REE patterns of the latter are similar to serpentinized peridotites measured at the Mid-Atlantic Ridge (Paulick et al., 2006).

A peridotite protolith for talc-magnesite samples is also consistent with their HSE abundances. The DSS bulk-rock HSE compositions are similar to some SOC dunites, both in relative and absolute abundances but are distinctly different from komatiites of similar MgO content, which have CaO and Al_2O_3 higher, and Pt and Pd lower, than in DSS samples (e.g., **Figure 2**). Compared to DSS samples, SOC peridotites are less serpentinized and did not experience steatitization (O'Driscoll et al., 2012). Studies have noted that, even under the highly-reducing conditions associated with serpentinization of abyssal and ophiolite peridotites, HSE mineral host phases remain relatively stable (Snow & Reisberg, 1996; Liu et al., 2009; Schulte et al., 2009). The HSE patterns measured in the DSS talc-magnesite samples are also similar to those of some peridotites from the Leka Ophiolite Complex (O'Driscoll et al., 2015), the ~90 Ma Troodos ophiolite (Büchl et al., 2004), the ~6 Ma Taitao ophiolite (Schulte et al., 2009), some abyssal peridotites (Liu et al., 2009), and orogenic massifs (e.g., Becker et al., 2006). Consequently, we argue that serpentinization or steatitization related removal of the HSE is minimal, with DSS talc-magnesite samples retaining mantle peridotite HSE compositions.

Osmium isotopic compositions of DSS talc-magnesite are also permissive with an origin as mantle peridotite. Average γOs value for the three samples is -3.0 ±0.7 (1 σ s.d.). This value is

lower than average initial γOs values for SOC harzburgites (-0.4 ±2.4; O'Driscoll *et al.*, 2012), but similar to average compositions of abyssal peridotites with >2 ppb Os (-1.7 ±4.3; 1 σ s.d.; n = 118; O'Driscoll et al., 2015), peridotites from the ~6 Ma Taitao Ophiolite (initial γOs value = -2.2 ±2.4; n = 22; Schulte *et al.*, 2009), and to Os-Ir-Ru alloy grains from the ~162 Ma Josephine Ophiolite (average initial γOs value = ~-1.4 ±6.5; n = 825; Meibom *et al.*, 2002; Walker *et al.*, 2005).

Our results imply that the protolith to the talc-magnesite samples and, therefore, the sample measured by Flinn & Moffat (1985) - as the same outcrops were sampled - were peridotites that experienced variable degrees of serpentinization and/or steatitization in an oceanic environment.

The nature and origin of the Dunrossness 'Spilites'

Flinn (1967) and Flinn & Moffat (1985) interpreted part of the ultramafic DSS to be a matrix-free serpentinized volcaniclastic breccia containing closely packed serpentine pseudomorphs that they considered to have replaced olivine spinifex texture. The DSS was considered to represent the eruption of basaltic and komatiitic lavas in an extensional basin. Flinn et al. (2013) interpreted the komatiitic compositions to result from 'total adiabatic melting' of the mantle due to instantaneous rifting of Laurentian lithosphere, followed by more typical partial melting to form basalts.

Komatiites are important for understanding secular cooling of the Earth, with high-MgO melts requiring either instantaneous adiabatic decompression, or high mantle potential temperatures (Viljoen & Viljoen, 1969; Arndt & Nisbet 1982). With two notable Phanerozoic exceptions (e.g., Arndt & Nesbitt, 1982; Hanski et al., 2004), the majority of komatiites in the geological record are Archaean. The interpretation of komatiite in the Neoproterozoic Dalradian rocks of southern Shetland has therefore not gone without dispute. Nesbitt & Hartmann (1986) noted that textures reported by Flinn & Moffat (1985) were similar to 'jack-straw' metamorphic textures observed in some serpentinized rocks. These authors also argued that compositions

reported by Flinn & Moffat (1985) for their 'komatiite' were too MgO-rich and TiO_2-poor to match any known spinifex-textured Archaean komatiite. Comparison of the Shetland talc-magnesite samples with Cretaceous and Archaean spinifex-textured komatiite illutstrates that the komatiites also have systematically higher Al_2O_3, CaO, V, Cu, Y, Zr, Nb and REE abundances (*Table* S2). Nesbitt & Hartman (1986) emphasised that, if the DSS rocks represented liquid compositions, their MgO contents were close to that of upper mantle peridotite. This would imply exceedingly high mantle potential temperatures.

Instead of a rift-basin origin for the DSS, an alternative model is an ophiolite origin (Garson & Plant., 1973; Nesbitt & Hartmann, 1986). The HSE systematics for the DSS talc-magnesite samples lends support to this model. One of the major impediments for a volcaniclastic origin for Flinn and co-workers was the presence of hornblende-bearing gabbros in the volcanic succession. An ophiolite mode-of-origin for the DSS would be consistent with recognized ophiolites, with the ultramafic units representing mantle or lower crustal section, with pillow lavas consistent with submarine eruption. Hornblende-bearing gabbros, in this scenario, would be equivalent to minor gabbroic crustal components. Similarly, the SOC has a pronounced lower crustal section, dominated by dunite and harzburgite, with gabbroic or wehrlitic bodies (e.g., Flinn & Oglethorpe, 2005).

An alternative origin for the DSS ultramafic portions is that they represent sub-continental lithospheric mantle (SCLM), protruded as serpentinite during extension associated with Dalradian basin formation. Similar models have been invoked to explain serpentinite 'olistoliths' in the Dalradian Supergroup elsewhere (Graham & Bradbury, 1981; Chew, 2001). The HSE abundance patterns and Os isotope compositions permit the DSS peridotite protoliths to be Neoproterozoic SCLM. However, as pointed out by Flinn & Moffat (1985), outcrop of the DSS is closely associated with a major positive Bouguer gravity anomaly (Tully & Howell, 1978) and with positive aeromagnetic anomalies (Howell, 1980) (**Figure 1**). This suggests that the DSS mafic and ultramafic rocks may extend to the east and northeast beneath the unconformably overlying Old Red Sandstone. The geophysical anomalies continue as far north as Unst, permitting a direct relationship between the SOC and the DSS. For this reason, we interpret the

DSS talc-magnesite rocks as altered oceanic peridotites, associated with the SOC, and not Neoproterozoic SCLM.

An important implication of our observations is that obduction of a much larger mass of oceanic lithosphere occurred than previously considered. A combined SOC and DSS would extend along strike for at least 90 km and constitute the most extensive ophiolite in the Scottish and Irish Caledonides. Field relations of the DSS permit an allochthonous origin, although the suggested obduction thrust must have been thoroughly reworked during development of the steep regional foliation within the Dalradian that occurred during the Grampian Orogeny (Walker et al. 2015). The suggestion of Flinn (2007) that the SOC originated in a marginal basin to the Iapetus Ocean was predicated on identification of the DSS ultramafic rocks as komatiites. On the basis of our data, there is no reason why the SOC cannot represent an oceanic core complex in a fore-arc environment, as proposed by Crowley & Strachan (2015). Study of the DSS as part of a larger mass of obducted lithosphere will likely help in eludicating formation environment models for the SOC and other Iapetan ophiolites.

Acknowledgements

We thank Martin Hole, Ambre Luguet, an anonymous reviewer, and the Subject Editor, Tyrone Rooney, for their constructive comments. This work was supported by the National Science Foundation (NSF EAR 1447130). BO'D acknowledges support from a Royal Society Research Grant (RG100528) and from Natural Environment Research Council (NERC) New Investigator grant NE/J00457X/1. JSD was supported by a UCD Seed Funding grant, which is gratefully acknowledged.

References

Alexander, E.B., 1988. Morphology, fertility and classification of productive soils on serpentinized peridotite in California (USA). Geoderma, 41, 337–351.

Anonymous, 1972. Penrose field conference on Ophiolites. Geotimes, 17, 24–25.

Arndt, N.T., Nisbet, E.G. (Eds.), 1982. Komatiites. George Allen and Unwin, London.

Becker, H., Horan, M.F., Walker, R.J., Gao, S., Lorand, J.-P., Rudnick, R.L., 2006. Highly siderophile element composition of the Earth's primitive upper mantle: Constraints from new data on peridotite massifs and xenoliths. Geochimica et Cosmochimica Acta 70, 4528-4550.

Büchl, A., Brügmann, G.E., Batanova, V.G., 2004. Formation of podiform chromitite deposits: implications from PGE abundances and Os isotopic compositions of chromites from the Troodos complex, Cyprus. Chemical Geology, 208, 217-232.

Chew, D.M., 2001. Basement protrusion origin of serpentinites in the Dalradian. Irish Journal of Earth Sciences 19, 23-35.

Coleman, R.G., 1977. Ophiolites. New York, SpringerVerlag, 220 p.

Connolly, B.D., Puchtel, I.S., Walker, R.J., Arevalo, R., Piccoli, P.M., Byerly, G., Robin-Popieul, C., Arndt, N., 2011. Highly siderophile element systematics of the 3.3 Ga Weltevreden komatiites, South Africa: implications for early Earth history. Earth and Planetary Science Letters 311, 253–263.

Crowley, Q.G., Strachan, R.A., 2015. U-Pb zircon constraints on obduction initiation of the Unst Ophiolite: an oceanic core complex in the Scottish Caledonides? Journal of the Geological Society, London 172, 279-282.

Dewey, J.F., Bird, J.M., 1971. The origin and emplacement of the ophiolite suite: Appalachian ophiolites in Newfoundland. Journal of Geophysical Research, 76, 3179–3206.

Dewey, J.F., Ryan, P.D., 1990. The Ordovician evolution of the South Mayo trough, western Ireland. Tectonics, 9, 887-901.

Dilek, Y., Furnes, H., 2011. Ophiolite genesis and global tectonics: geochemical and tectonic fingerprinting of ancient oceanic lithosphere. Geological Society of America Bulletin, 123, 387-411.

Flinn, D., 1967. The metamorphic rocks of the southern part of the Mainland of Shetland. Geological Journal, 5, 251-290.

Flinn, D., 2007. The Dalradian rocks of Shetland and their implications for the plate tectonics of the northern Iapetus. Scottish Journal of Geology, 43, 125-142.

Flinn, D., Moffat, D.T., 1985. A peridotitic komatiite from the Dalradian of Shetland. Geological Journal, 20, 287-292.

Flinn, D., Moffat, D.T., 1986. A reply to RW Nesbitt and LA Hartmann. Geological Journal, 21, 207-209.

Flinn, D., Oglethorpe, R.J.D., 2005. A history of the Shetland Ophiolite Complex. Scottish Journal of Geology, 41,141–148.

Flinn, D., May, F., Roberts, J.L., Treagus, J.E., 1972. A revision of the stratigraphic succession of the East Mainland of Shetland. Scottish Journal of Geology, 8, 335-343.

Flinn, D., Stone, P., Stephenson, D., 2013. The Dalradian rocks of the Shetland Islands, Scotland. Proceedings of the Geologists' Association, 124, 393-409.

Garson, M.S., Plant, J., 1973. Alpine type ultramafic rocks and episodic mountain building in the Scottish Highlands. Nature Physical Science 242, 34–38.

Graham, C.M., Bradbury, H.J., 1981. Cambrian and late Precambrian basaltic igneous activity in the Scottish Dalradian: a review. Geological Magazine 118(1), 27-37.

Howell, P.M., 1980. Aeromagnetic Anomaly Map of Shetland (1:250000), Sheet 60°N-2°W. Institute of Geological Sciences, London. Crown Copyright.

Janecky, D.R., Seyfried Jr., W.E., 1986. Hydrothermal serpentinization of peridotite within the oceanic crust: Experimental investigations of mineralogy and major element chemistry. Geochimica et Cosmochimica Acta, 50, 1357 1378.

Liu, C.-Z., Snow, J.E., Brügmann, G., Hellebrand, E., Hofmann, A.W., 2009. Non-chondritic HSE budget in Earth's upper mantle evidenced by abyssal peridotites from Gakkel ridge (Arctic Ocean). Earth and Planetary Science Letters, 283, 122–132.

Meibom, A., Sleep, N.H., Chamberlain, C.P., Coleman, R.G., Frei, R., Hren, M.T., Wooden, J. L., 2002. Re-Os isotopic evidence for long-lived heterogeneity and equilibration processes in the Earth's upper mantle. Nature, 419, 705-708.

Nesbitt, R.W., Hartmann, L.A., 1986. Comments on 'a peridotitic komatiite from the Dalradian of Shetland' by D. Flinn and DT Moffat. Geological Journal, 21, 201-205.

Nicolas, A., 1989. Structure of Ophiolites and Dynamics of Oceanic Lithosphere. Dordrecht, the Netherlands, Kluwer Academic Publishers, 367 p.

O'Driscoll, B., Day J.M.D., Walker R.J., Daly J.S., McDonough W.F., Piccoli P.M., 2012. Chemical heterogeneity in the upper mantle recorded by peridotites and chromitites from the Shetland Ophiolite Complex, Scotland. Earth and Planetary Science Letters, 333-334, 226-237.

O'Driscoll, B., Walker, R.J., Day, J.M.D., Ash, R.D., Daly, J.S., 2015. Generations of Melt Extraction, Melt–Rock Interaction and High-Temperature Metasomatism Preserved in Peridotites of the~ 497 Ma Leka Ophiolite Complex, Norway. Journal of Petrology, 56, 1797-1828.

Paulick, H., Bach, W., Godard, M., De Hoog, J.C.M., Suhr, G., Harvey, J., 2006. Geochemistry of abyssal peridotites (Mid-Atlantic Ridge, 15 20′ N, ODP Leg 209): implications for fluid/rock interaction in slow spreading environments. Chemical Geology, 234, 179-210.

Schulte, R.F., Schilling, M., Horan, M.F., Anma, R., Komiya, T., Farquhar, J., Piccoli, P.M., Pitcher, L., Walker, R.J., 2009. Chemical and chronologic complexity in the convecting upper mantle: evidence from the Taitao Ophiolite, southern Chile. Geochimica et Cosmochimica Acta, 73, 5793-5819.

Snow, J.E., Dick, H.J.B., 1995. Pervasive magnesium loss by marine weathering of peridotite. Geochimica et Cosmochimica Acta, 59, 4219–4235.

Snow, J.E., Reisberg, L., 1995. Os isotopic systematics of the MORB mantle: results from altered abyssal peridotites. Earth and Planetary Science Letters, 133, 411-421.

Spray, J.G., Dunning, G.R., 1991. A U/Pb age for the Shetland Islands oceanic fragment, Scottish Caledonides: evidence from anatectic plagiogranites in 'layer 3' shear zones. Geological Magazine 128, 667-671.

Strachan, R.A., Harris, A.L., Fettes, D.J., Smith, M., 2002. The Northern Highland and Grampian terranes. In: Trewin, N.H. (Ed.), The Geology of Scotland., Fourth Edition. The Geological Society, London, 81–148.

Strachan, R.A., Prave, A.R., Kirkland, C.L., Storey, C.D., 2013. U-Pb detrital zircon geochronology of the Dalradian Supergroup, Shetland Islands, Scotland: Implications for

regional correlations and Neoproterozoic-Palaeozoic basin development. Journal of the Geological Society, London, 170, 905-916.

Sun, S.S., McDonough, W.S., 1989. Chemical and isotopic systematics of oceanic basalts: implications for mantle composition and processes. Geological Society, London, Special Publications, 42, 313-345.

Tully, M.C., Howell, P.M., 1978. Bouguer Gravity Anomaly Map of Shetland (1:250000), Sheet 60°N-2°W. Institute of Geological Sciences, London. Crown Copyright.

Viljoen, M.J., Viljoen, R.P., 1969. Evidence for the existence of a mobile extrusive peridotite magma from the Komati Formation of the Onverwacht Group. Geological Society of South Africa, Special Publication, 2, 87–112.

Walker, R.J., Brandon, A.D., Bird, J.M., Piccoli, P.M., McDonough W.F., Ash R.D., 2005. ^{186}Os-^{187}Os systematics of Os-Ir-Ru alloy grains, southwestern Oregon. Earth and Planetary Science Letters, 230, 211-226.

Walker, S., Thirlwall, M.F., Strachan, R.A., Bird, A.F., 2015. Evidence from Rb-Sr mineral ages for multiple orogenic events in the Caledonides of Shetland, Scotland. Journal of the Geological Society. doi:10.1144/jgs2015-034.

Figures and figure captions

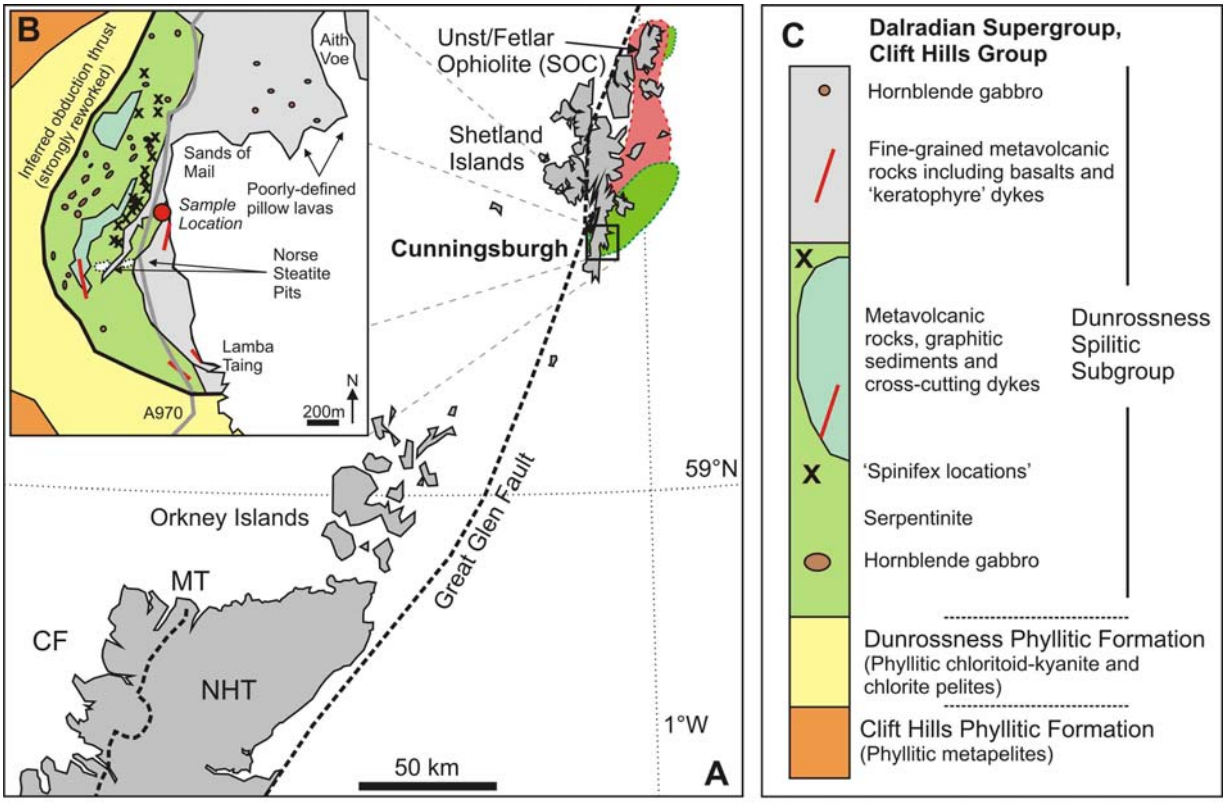

Figure 1 – (a) Map of northern Scotland, the Orkney and Shetland Islands, showing the locations of the Shetland ophiolite complex (SOC), on Unst and Fetlar, and the Cunningsburgh area shown in detail in (b). CF = Caledonian Foreland; MT = Moine Thrust; NHT = Northern Highland Terrane. Green and red shaded regions illustrate the aeromagnetic (~300 nT contour) and bouguer gravity anomalies (~25 mGal contour), respectively (Tully & Howell, 1978; Howell, 1980), noted by Flinn & Moffat (1985). (b) Simplified geological map showing the sample locations used in this study, as well as the locations of 'spinifex-textures' (X) identified within the serpentinized and steatitized Dunrossness Spilitic Subgroup by Flinn & Moffat (1985) and Flinn et al. (2013). (c) Idealised stratigraphic section, modified from Flinn et al. (2013), of the Dalradian Supergroup in the region of map (b).

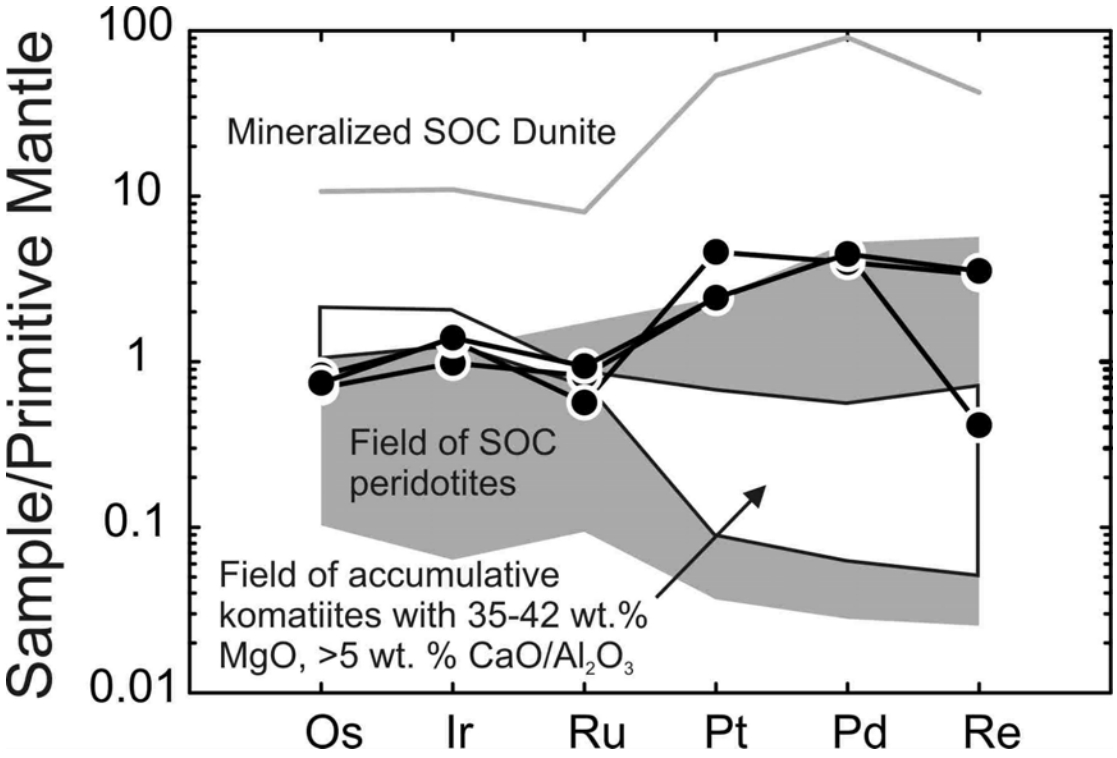

Figure 2 - Primitive mantle normalized highly siderophile element patterns for talc-magnesite samples from South Shetland (filled circles), compared with peridotites (dunite and harzburgite) from the SOC from O'Driscoll et al. (2012) and high-MgO cumulates from the Weltevreden komatiites (Connolly et al., 2011). Primitive mantle normalization from Becker et al. (2006).

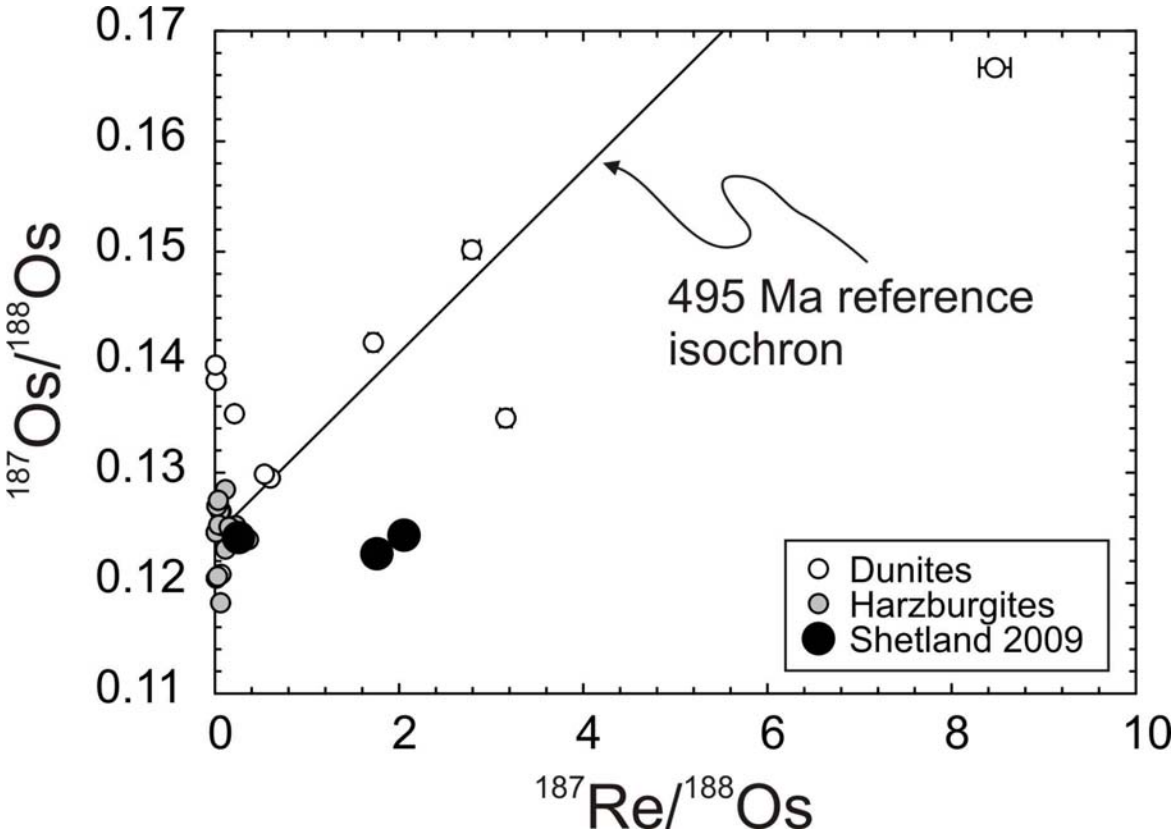

Figure 3 - $^{187}Re/^{188}Os$-$^{187}Os/^{188}Os$ diagram for talc-magnesite samples from south Shetland, compared with dunite and harzburgite samples from the ~495 Ma SOC (Spray & Dunning, 1991) on Unst and Fetlar from O'Driscoll et al. (2012). Shown is a 495 Ma reference isochron anchored to an initial $^{187}Os/^{188}Os$ ratio of 0.1243.

Supplementary Information for: **Identification of mantle peridotite and a possible Iapetan ophiolite sliver in south Shetland, Scottish Caledonides**

Supplementary Methods

Major element compositions were measured by X-ray fluorescence (XRF) at Franklin and Marshall College using a *PW 2404 PANalytical XRF* vacuum spectrometer following the procedures outlined in Boyd & Mertzman (1987). Precision and accuracy for the average of 13 runs of BHVO-2 relative to USGS accepted values is estimated at <0.2% for SiO_2 and TiO_2, <1% for Al_2O_3, MgO, Fe_2O_{3T}, CaO, Na_2O, P_2O_5, and <3% for K_2O. Trace-element abundances were determined at the *Scripps Isotope Geochemistry Laboratory (SIGL)*, with a *Thermo Scientific iCAPq* quadrupole inductively coupled plasma mass spectrometer, using methods described previously in Day et al. (2014). Samples were prepared with international and internal rock standards (BHVO-2, BIR-1, BCR-2, AGV-2, DTS-2b, GP-13). Reproducibility of the basaltic reference materials was generally better than 5% (RSD), and 10% (RSD) for peridotite standards.

Osmium isotope and HSE abundance analyses were performed at the *SIGL*. Homogenised powder aliquots were prepared along with total analytical blanks and were digested in sealed borosilicate Carius tubes, with isotopically enriched multi-element spikes (^{99}Ru, ^{106}Pd, ^{185}Re, ^{190}Os, ^{191}Ir, ^{194}Pt), and 11 mL of a 1:2 mixture of Teflon-distilled HCl and HNO_3 that was purged of Os by reaction with H_2O_2. Samples were digested to a maximum temperature of 270˚C in an oven for 72 hours. Osmium was triply extracted from the acid using CCl_4 and then back-extracted into HBr (Cohen & Waters, 1996), prior to purification by micro-distillation (Birck et al., 1997). Rhenium and the other HSE were recovered and purified from the residual solutions using standard anion exchange separation techniques. Measurement protocols were identical to those described previously (e.g., Day et al., 2016). Isotopic compositions of Os were measured in negative-ion mode on a *ThermoScientific Triton* thermal ionisation mass spectrometer at the *SIGL*. Rhenium, Pd, Pt, Ru and Ir were measured using an *Cetac Aridus II* desolvating nebuliser coupled to a *ThermoScientific iCAPq* ICP-MS. Offline corrections for Os involved an oxide correction, an iterative fractionation correction using ^{192}Os/^{188}Os = 3.08271, a ^{190}Os spike

subtraction, and finally, an Os blank subtraction. Precision for $^{187}Os/^{188}Os$, determined by repeated measurement of the UMCP Johnson-Matthey standard was better than ±0.2% (2 St. Dev.; 0.11390 ±20; n = 5). Measured Re, Ir, Pt, Pd and Ru isotopic ratios for sample solutions were corrected for mass fractionation using the deviation of the standard average run on the day over the natural ratio for the element. External reproducibility on HSE analyses using the *iCAPq* was better than 0.5% for 0.5 ppb solutions and all reported values are blank-corrected. The total analytical blanks (n = 3) run with the samples had $^{187}Os/^{188}Os$ = 0.401 ± 0.010, with quantities (in picograms) of 4.2 ±1.3 [Re], 2.8 ±0.3 [Pd], 2.0 ±0.9 [Pt], 13.3 ±1.3 [Ru], 0.3 ±0.2 [Ir] and 0.2 ±0.1 [Os]. These blanks resulted in negligible corrections to samples (<1%).

Supplementary Discussion

Steatized rocks in the DSS have been recognized for some time, and were exploited by the Norse during their occupation of Shetland, for the manufacture of utensils (e.g., Jones et al., 2007). The anhydrous bulk-composition of the DSS talc-magnesite samples is similar to that of peridotite that has otherwise experienced extensive serpentinization and metasomatism. The bulk composition of the sample in this study, which has been steatitized and serpentinized, is broadly similar to that of the sample reported in Flinn & Moffat (1985), which was reportedly not steatitized. One principal difference is that the steatitized sample analysed in this study has much lower Mg. We suggest that this difference is due to Mg-loss or Si-gain (Malvoisin, 2015) during localized steatitization within the DSS ultramafic rocks. In the case of the DSS, alteration probably occurred in two distinct episodes. First, by serpentinisation of olivine in the reaction of forsterite → serpentine + brucite, idealized as:

$$2Mg_2SiO_4 + 3H_2O \rightarrow Mg_3Si_2O_5(OH)_4 + Mg(OH)_2$$

Or through Si metasomatism in the reaction:

$$3Mg_2SiO_4 + 4H_2O + SiO_2\ aq \rightarrow 2Mg_3Si_2O_5(OH)_4$$

Followed by the carbonation of serpentine to form talc-magnesite, in the reaction:

$$2Mg_3Si_2O_5(OH)_4 + 3CO_2 \rightarrow Mg_3Si_4O_{10}(OH)_2 + 3MgCO_3 + 3H_2O$$

Relative reduction in the Mg/Si and Al/Si ratios of peridotites has previously been demonstrated to occur during Si metasomatism (Paulick et al., 2006), although in the Dunrossness examples the low Mg in steatitized samples also leads to the possibility that loss of Mg occurred during carbonate metasomatism. The bulk compositions of our sample and that of Flinn & Moffat (1985) are therefore consistent with a peridotite protolith, an observation that is supported by the similarity in bulk composition observed between the DSS ultramafic rocks, and ultramafic rocks preserved in the SOC on Unst and Fetlar. Enrichments in Sr, Ba, Pb, U and Cs, the light REE and Eu all indicate extensive seafloor alteration of the talc-magnesite samples. The REE patterns measured in the talc-magnesite samples are similar to some serpentinized peridotites measured at the Mid-Atlantic Ridge. It has been demonstrated that vent fluids enriched in the LREE and Eu pervasively altered serpentinized peridotites at the Mid-Atlantic Ridge, 15°20′N, ODP Leg 209 (Paulick et al., 2006). In this circumstance, alteration began with serpentinization at 100-200°C under seawater-like pH values, followed by higher-temperature interactions at 300-400°C, with low pH (4-5) (e.g., Paulick et al., 2006).

The results strongly imply that the protolith to the talc-magnesite samples and, therefore, the sample measured by Flinn & Moffat (1985) - as the same outcrops were sampled - were peridotites that experienced variable degrees of serpentinization and/or steatitization in an oceanic environment. Based on prior studies of modern abyssal peridotites, most of the alteration experienced by the protoliths in the DSS could have occurred at a paleo- ridge setting, with no particular requirement for later alteration. Due to the extreme degrees of alteration of samples, it is difficult to ascertain if the protoliths were harburgite or dunite. The current data are permissive of dunitic protoliths, similar to those that make up variably thick (up to 10 m) channels and lenses in the harzburgitic mantle and the bulk of the lower crustal cumulate section in the SOC (e.g., Prichard, 1985; Flinn & Oglethorpe, 2005). Accessory Cr-spinel, usually relatively resistant to low-temperature modification, exhibits widespread alteration to more brightly reflective ferroan Cr-spinel. The ferroan Cr-spinel occurs as ragged rims on primary grains and within intra-grain

microfractures. These complex alteration textures indicate there is comparatively little primary Cr-spinel remaining in the DSS samples.

In *Table S1* we report present-day γ_{Os} values (-2.5 to -3.8) and rhenium depletion (T_{RD}) ages (or minimum melt depletion ages) of 0.7 to 1 Ga, assuming chondritic mantle evolution (after Shirey & Walker, 1998). These are similar to γ_{Os} values and T_{RD} ages reported for some SOC harzburgites and dunites (O'Driscoll et al., 2012). Assuming a similar Iapetus-aged heritage for the talc-magnesite samples from south Shetland, to the SOC, we also report γ_{Os} values at 495 Ma – the reported age of the SOC (Spray & Dunning, 1991). The γ_{Os} values at 495 Ma range from -1.9 to -13.6. The low γ_{Os} values likely reflect addition of Re after formation of the talc-magnesite samples as harzburgites or dunites, with addition of Re occurring during hydrothermal alteration.

Supplementary References

Birck, J.-L., Roy-Barman, M., and Capmas, F., 1997. Re-Os isotopic measurements at the femtomole level in natural samples. Geostandards Newsletter, 21, 21-28.

Boyd, F.R., Mertzman, S.A., 1987. Composition and structure of the Kaapvaal lithosphere, southern Africa. In: Mysen, B.O. (Ed.) Magmatic processes – physiochemical principles. Geochemical Society Special Publications, 1, 13-24.

Cohen, A.S., Waters, F.G., 1996. Separation of osmium from geological materials by solvent extraction for analysis by thermal ionisation mass spectrometry. Analytica Chimica Acta, 332, 269-275.

Day J.M.D., Peters B.J., Janney P.E., 2014. Oxygen isotope systematics of South African olivine melilitites and implications for HIMU mantle reservoirs. Lithos, 202-203, 76-84.

Day J.M.D., Waters C. L., Schaefer B. F., Walker R. J., Turner, S., 2016. Use of Hydrofluoric acid desilicification in the determination of highly siderophile element abundances and Re-Pt-Os isotope systematics in mafic-ultramafic Rocks. Geostandards and Geoanalytical Research. 40, 49-65.

Flinn, D., Moffat, D.T., 1985. A peridotitic komatiite from the Dalradian of Shetland. Geological Journal, 20, 287-292.

Jones, R.E., Kilikoglou, V., Olive, V., Bassiakos, Y., Ellam, R., Bray, I.S.J., Sanderson, D.C.W., 2007. A new protocol for the chemical characterisation of steatite – two case studies in Europe: the Shetland Islands and Crete. Journal of Archaeological Science, 34, 626-641.

Paulick, H., Bach, W., Godard, M., De Hoog, J.C.M., Suhr, G., Harvey, J., 2006. Geochemistry of abyssal peridotites (Mid-Atlantic Ridge, 15 20′ N, ODP Leg 209): implications for fluid/rock interaction in slow spreading environments. Chemical Geology, 234, 179-210.

Puchtel, I.S., Blichert-Toft, J., Touboul, M., Walker, R.J., Byerly, G., Nisbet, E.G., Anhaeusser, C.R., 2013. Insights into early Earth from Barberton komatiites: evidence from lithophile isotope and trace element systematics. Geochimica et Cosmochimica Acta, 108, 63-90.

Prichard, H.M., 1985, The Shetland Ophiolite. In: Gee, D.G., Sturt, B.A. (Eds.) The Caledonide orogen: Scandinavia and related areas: Wiley and Sons, V. 2, p. 1173−1184.

Malvoisin, B., 2015. Mass transfer in the oceanic lithosphere: Serpentinization is not isochemical. Earth and Planetary Science Letters, 430, 75–85.

Revillon, S., Arndt, N.T., Chauvel, C., Hallot, E., 2000. Geochemical study of ultramafic volcanic and plutonic rocks from Gorgona Island, Columbia: The plumbing system of an oceanic plateau. Journal of Petrology, 41, 1127-1153.

Shirey, S.B., Walker, R.J., 1998. The Re-Os isotope system in cosmochemistry and high-temperature geochemistry. Ann. Rev. Earth Planet. Sci. 26, 423-500.

Spray, J.G., Dunning, G.R., 1991. A U/Pb age for the Shetland Islands oceanic fragment, Scottish Caledonides: evidence from anatectic plagiogranites in ‘layer 3’ shear zones. Geological Magazine 128, 667-671.

Sun, S.S. and McDonough, W.S., 1989. Chemical and isotopic systematics of oceanic basalts: implications for mantle composition and processes. Geological Society, London, Special Publications, 42(1), pp.313-345.

Supplementary Figures

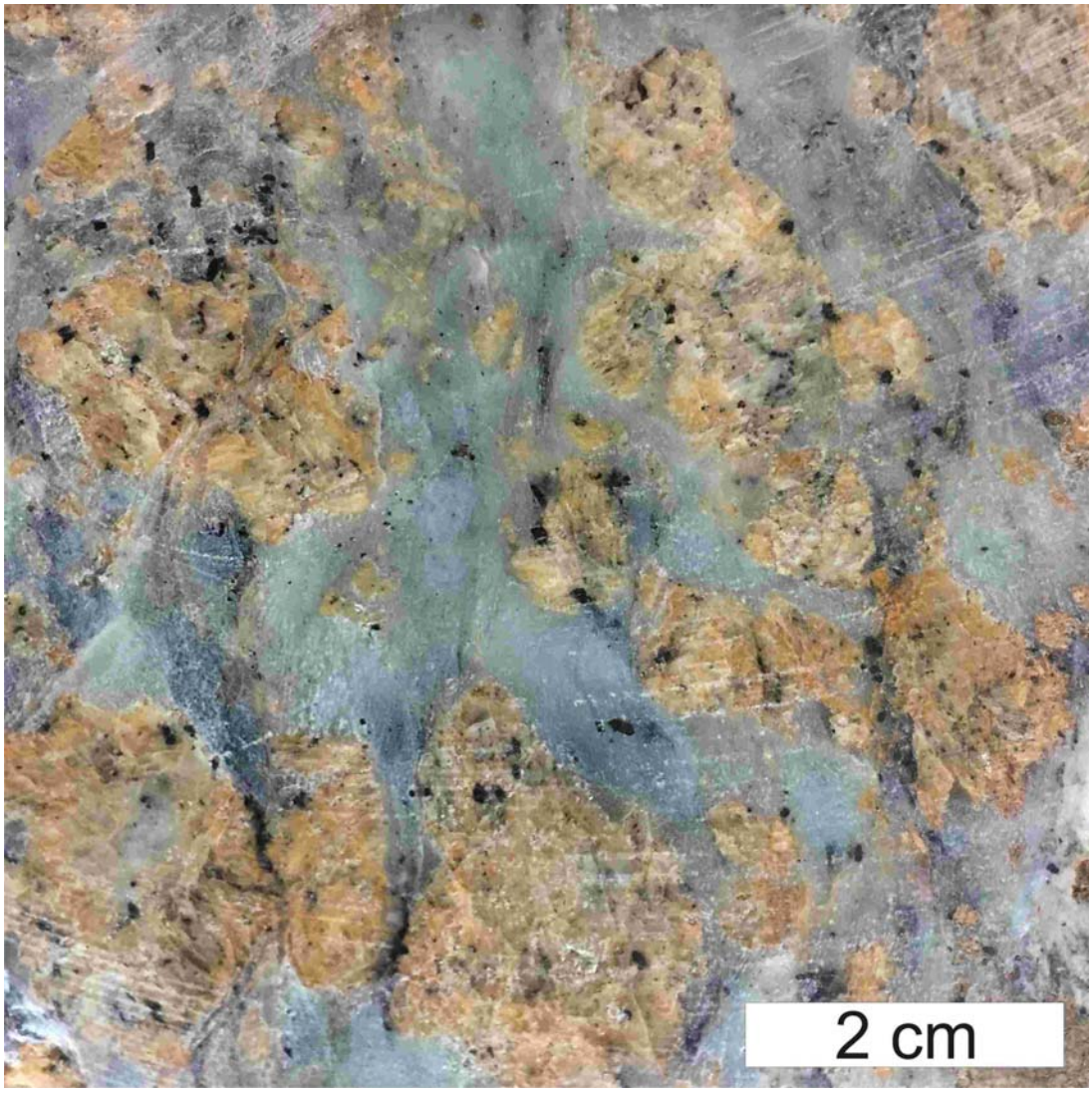

Figure S1 - Photograph of a slab-cut of one of the samples analysed in this study. The sample is a talc-magnesite metamorphic assemblage, representing the reaction of forsterite → serpentine + brucite, followed by carbonation of serpentine to form talc-magnesite. Magnesites are large orange-brown multi-crystalline masses within blue-green talc. Black grains are Cr-spinel, or alteration minerals after Cr-Spinel. Secondary pyrite is also visible in some portions of the samples.

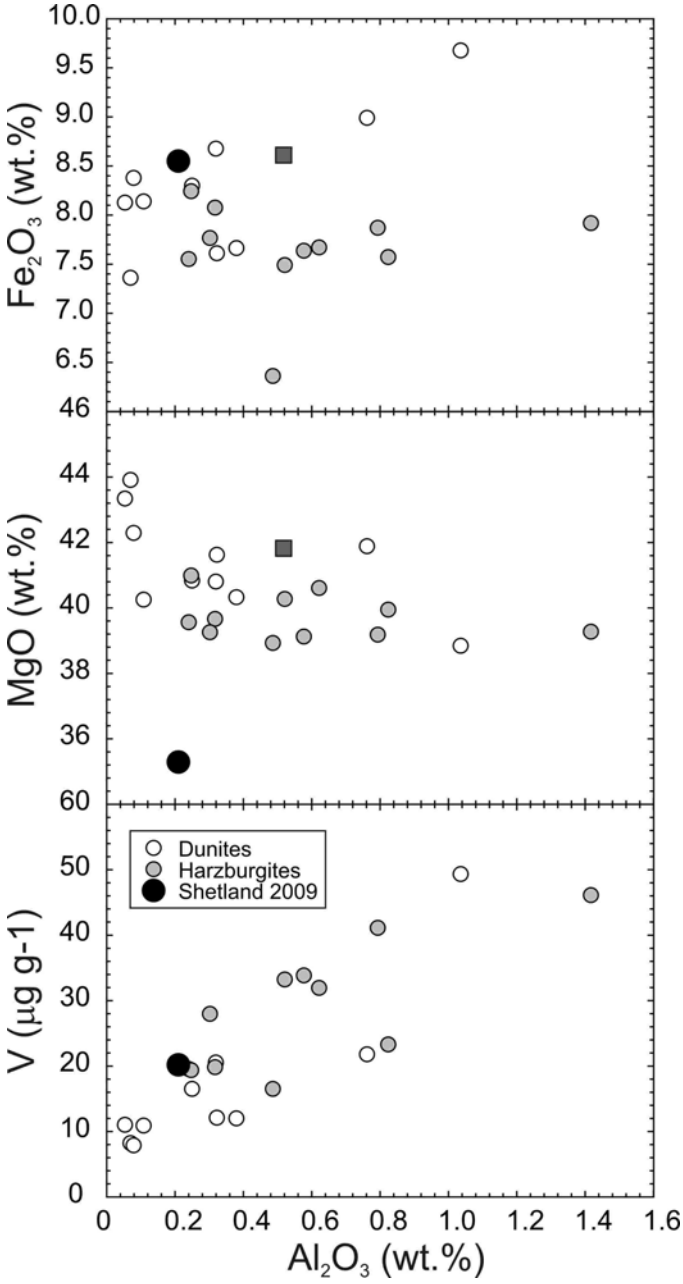

Figure S2 - Plots of Al_2O_3 versus Fe_2O_3, MgO and V for talc-magnesite samples from south Shetland (Shetland 2009), versus dunite and harzburgite compositions measured for the SOC, on Unst and Fetlar, from O'Driscoll et al. (2012). Also shown is the composition of the 'Dalradian komatiite' composition (filled square) from Flinn & Moffat (1985).

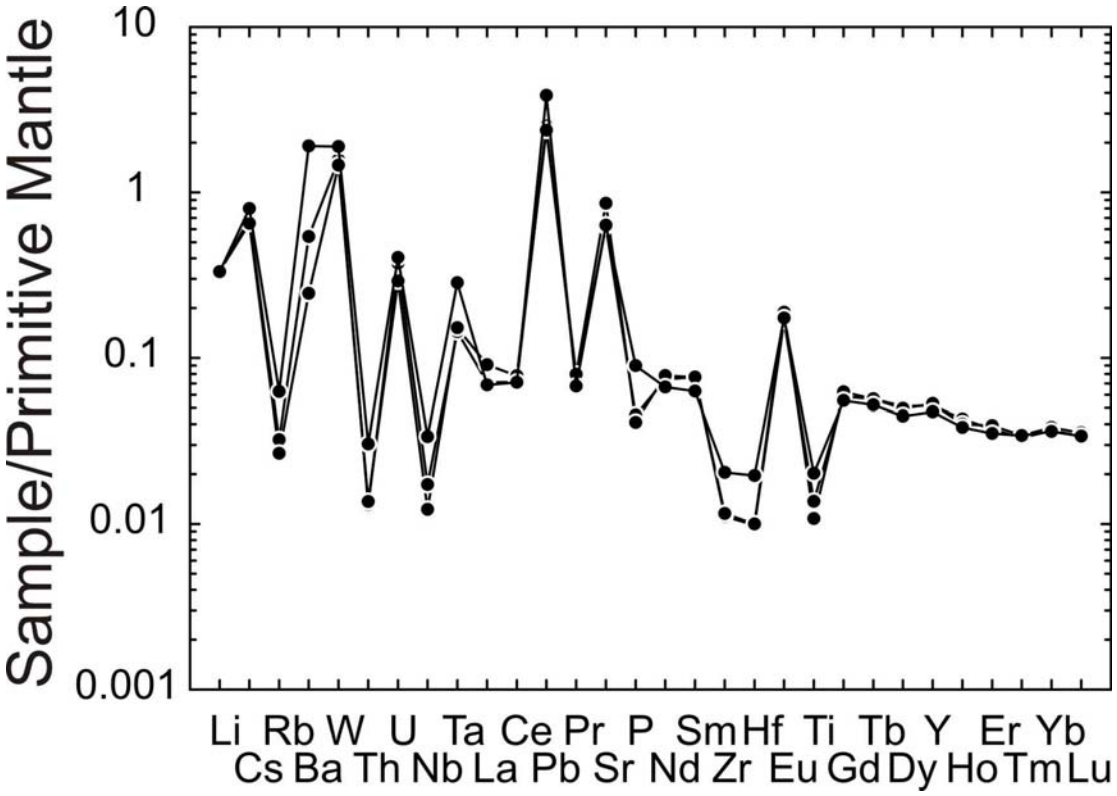

Figure S3 - Incompatible trace element patterns for talc-magnesite samples from South Shetland, normalized to a primitive mantle composition (Sun & McDonough, 1989), with increasing compatibility to the right.

Table S1 - Compositions of talc-magnesite samples from south Shetland

Major-element composition (wt.% oxides and $\mu g\ g^{-1}$ for Cr, Ni, Co and Ga)

	SiO_2	TiO_2	Al_2O_3	Fe_2O_{3T}	MnO	MgO	CaO	Na_2O	K_2O	P_2O_5	Total	LOI		FeO	Fe_2O_3		Co	Ni	Cr	Ga
S 2009 a	53.62	<0.01	0.21	8.55	0.21	35.29	1.61	0.1	<0.01	0.01	99.6	19.65		4.16	3.93		85	2395	3378	2.4
FM1985	*46.42*	*0.09*	*0.52*	*8.61*	*0.21*	*41.82*	*2.49*	*<0.01*	*0.05*	*0.02*	*100.2*							*2200*	*2400*	

Trace-element abundances (in $\mu g\ g^{-1}$)

	Li	B	P	Sc	Ti	V	Cr	Mn	Co	Ni	Cu	Zn	Ga	Ge	Rb	Sr	Y	Zr	Nb	Cs
S 2009 a	1.43	0.34	4.3	3.13	17.81	20.17	3746	1094	79.21	1592	5.80	60.54	2.41	0.78	0.021	13.18	0.24	0.12	0.0123	0.0222
S 2009 b	1.44	0.29	3.9	3.04	14.00	12.25	1408	1159	84.09	1601	6.40	28.56	1.79	0.73	0.017	18.13	0.24	0.13	0.0087	0.0208
S 2009 c	1.43	0.26	8.5	3.03	26.30	11.89	1442	1092	79.16	1608	7.60	33.89	1.81	0.72	0.040	13.38	0.22	0.23	0.0240	0.0255

	Ba	La	Ce	Pr	Nd	Sm	Eu	Gd	Tb	Dy	Ho	Er	Tm	Yb	Lu	Hf	Ta	W	Pb	Th	U
S 2009 a	3.78	0.0489	0.1270	0.0208	0.1005	0.0341	0.0281	0.0349	0.0061	0.0377	0.0071	0.0179	0.0025	0.0181	0.0025	0.0030	0.0059	0.031	0.47	0.0011	0.0078
S 2009 b	1.71	0.0624	0.1385	0.0220	0.1058	0.0340	0.0317	0.0371	0.0061	0.0365	0.0066	0.0188	0.0025	0.0188	0.0026	0.0031	0.0062	0.029	0.44	0.0012	0.0061
S 2009 c	13.31	0.0471	0.1261	0.0186	0.0902	0.0279	0.0293	0.0330	0.0056	0.0329	0.0063	0.0169	0.0025	0.0178	0.0025	0.0061	0.0117	0.038	0.71	0.0026	0.0085

Re-Os isotopes and HSE abundances (in ng g^{-1})

	Re	Pd	Pt	Ru	Ir	Os	$^{187}Re/^{188}Os$		$^{187}Os/^{188}Os$		γOs_{495Ma}	γOs	TRD (Ga)		Pd/Os	Pt/Os	Ru/Os	Ir/Os
S 2009 a	0.14	32.00	18.33	5.76	3.44	2.71	0.257	0.004	0.12411	0.00014	-1.9	-2.7	0.8		11.8	6.8	2.1	1.3
Blk %	*1.9%*	*0.6%*	*0.2%*	*2.4%*	*0.5%*	*0.1%*												
S 2009 b	1.18	28.28	34.93	3.96	4.69	3.23	1.758	0.026	0.12266	0.00008	-13.0	-3.8	1.0		8.8	10.8	1.2	1.5
Blk %	*0.2%*	*0.7%*	*0.1%*	*3.6%*	*0.4%*	*0.1%*												
S 2009 c	1.23	31.74	18.50	6.57	4.89	2.90	2.053	0.031	0.12433	0.00012	-13.6	-2.5	0.7		11.0	6.4	2.3	1.7
Blk %	*0.2%*	*0.6%*	*0.2%*	*2.0%*	*0.3%*	*0.1%*												

FM1985 - Data from Flinn & Moffat (1985); $\gamma Os = ([^{187}Os/^{188}Os_{sample}(t)/^{187}Os/^{188}Os_{chondrite}(t)] -1) \times 100$; $T_{RD} = 1/\lambda \times \ln\{([^{187}Os/^{188}Os_{chondrite} - {}^{187}Os/_{188}Os_{sample}]/ {}^{187}Re/^{188}Os_{chondrite}) + 1\}$

Table S2 - Comparison of South Shetland samples with Cretaceous and Archaean age spinifex komatiite

	Location	Age	SiO_2	TiO_2	Al_2O_3	Fe_2O_{3T}	MnO	MgO	CaO	Na_2O	K_2O	P_2O_5	Total	LOI		Co	Ni	Cr	V	Cu	Zn	Ga	Rb	Sr	Y
			wt.%	wt.%	wt.%	wt.%	wt.%	wt.%	wt.%	wt.%	wt.%	wt.%				ppm	ppm	ppm	ppm	ppm	ppm	ppm	ppm	ppm	ppm
S 2009 a	Shetland	Neoproterozoic	53.6	<0.01	0.21	8.55	0.21	35.3	1.61	0.1	<0.01	0.01	99.6	19.65		85	2395	3378	14.77	6.60	41.00	2.00	0.026	14.90	0.23
FM1985	Shetland	Neoproterozoic	46.4	0.09	0.52	8.61	0.21	41.8	2.49	<0.01	0.05	0.02	100.2				*2200*	*2400*							
GOR502	Gorgona	Cretaceous	46.1	0.74	13.1	12.6	0.20	14.5	11.4	1.26	0.04	0.04	100.0	3.28		69	520	1076	253	121	69	14	0.93	58.5	15
GOR525	Gorgona	Cretaceous	44.6	0.64	11.2	12.7	0.20	20.1	9.88	0.68	0.03	0.04	100.0	5.19		80	956	5614	162	99	66	12	1.17	66.39	12
GOR539	Gorgona	Cretaceous	44.5	0.62	10.6	12.2	0.19	21.0	10.1	0.85	0.05	0.04	100.0	5.56		81	1039	1297	207	94	63	11	0.61	91.14	12
BV05	Komati Fm.	Archaean	46.8	0.38	4.02	12.9	0.23	28.2	6.34	0.34	0.06	0.04	99.3	6.23		117	1560	2185	130		62.8	4.24			8.59
BV08	Komati Fm.	Archaean	47.0	0.40	4.09	12.9	0.20	27.8	6.66	0.32	0.02	0.05	99.4	6.44		107	1592	2139	134		61.3	4.37			8.73
SA564-4	Komati Fm.	Archaean	47.7	0.20	5.83	9.96	0.17	28.8	6.57	0.08	0.10	0.02	99.4	7.89		98.4	1396	2430	120		35.7	3.52			4.31
SA564-5	Komati Fm.	Archaean	47.8	0.17	5.08	10.1	0.14	31.3	4.65	0.08	0.09	0.02	99.4	8.42		97.8	1608	2559	103		33.4	3.2			3.94
KBA12-2	Komati Fm.	Archaean	48.0	0.20	5.70	10.8	0.16	28.9	5.37	0.08	0.08	0.02	99.3	8.08		100	1445	2772	125		46.8	3.77			4.48

	Location	Age	Zr	Nb	Cs	Ba	La	Ce	Pr	Nd	Sm	Eu	Gd	Tb	Dy	Ho	Er	Tm	Yb	Lu	Hf	Ta	Pb	Th	U
			ppm	ppm	ppm	ppm	ppm	ppm	ppm	ppm	ppm	ppm	ppm	ppm	ppm	ppm	ppm	ppm	ppm	ppm	ppm	ppm	ppm	ppm	ppm
S 2009 a	Shetland	Neoproterozoic	0.16	0.0150	0.0228	6.27	0.0528	0.1305	0.0205	0.0988	0.0320	0.0297	0.0350	0.0060	0.036	0.0066	0.0179	0.0025	0.0183	0.0026	0.0041	0.0079	0.54	0.0016	0.0075
FM1985	Shetland	Neoproterozoic																							
GOR502	Gorgona	Cretaceous	32	0.45	0.02	3.02	0.66	2.32	0.48	3.09	1.4	0.65	2.34	0.43	3.01	0.62	1.74	0.24	1.49	0.24	1.04	0.03	0.18	0.04	0.02
GOR525	Gorgona	Cretaceous	28	0.38	0.01	2.74	0.53	1.92	0.39	2.52	1.15	0.53	1.86	0.34	2.37	0.49	1.36	0.19	1.19	0.19	0.83	0.03	0.15	0.03	0.01
GOR539	Gorgona	Cretaceous	27	0.37	0.01	7.75	0.52	1.94	0.39	2.54	1.16	0.51	1.86	0.33	2.3	0.48	1.31	0.18	1.14	0.18	0.82	0.03	0.09	0.03	0.01
BV05	Komati Fm.	Archaean	25.3	1.67			1.94	5.52		3.94	1.16	0.396	1.48		1.52		0.892		0.837	0.122	0.733	0.117		0.193	0.038
BV08	Komati Fm.	Archaean	25.8	1.72			1.97	5.62		4.06	1.2	0.377	1.52		1.57		0.921		0.855	0.125	0.764	0.12		0.195	0.039
SA564-4	Komati Fm.	Archaean	9.53	0.34			0.338	0.972		0.853	0.324	0.122	0.514		0.68		0.467		0.493	0.078	0.236	0.02		0.024	0.008
SA564-5	Komati Fm.	Archaean	8.48	0.32			0.326	0.922		0.797	0.303	0.124	0.472		0.62		0.431		0.457	0.072	0.221	0.019		0.022	0.008
KBA12-2	Komati Fm.	Archaean	9.57	0.34			0.37	1.02		0.888	0.335	0.111	0.533		0.72		0.498		0.518	0.083	0.247	0.02		0.024	0.008

Gorgona data from Revillion et al. (2000). Komati Fm. Data from Puchtel et al. (2013).